

Nanoscale

Accepted Manuscript



This is an *Accepted Manuscript*, which has been through the Royal Society of Chemistry peer review process and has been accepted for publication.

Accepted Manuscripts are published online shortly after acceptance, before technical editing, formatting and proof reading. Using this free service, authors can make their results available to the community, in citable form, before we publish the edited article. We will replace this *Accepted Manuscript* with the edited and formatted *Advance Article* as soon as it is available.

You can find more information about *Accepted Manuscripts* in the [Information for Authors](#).

Please note that technical editing may introduce minor changes to the text and/or graphics, which may alter content. The journal's standard [Terms & Conditions](#) and the [Ethical guidelines](#) still apply. In no event shall the Royal Society of Chemistry be held responsible for any errors or omissions in this *Accepted Manuscript* or any consequences arising from the use of any information it contains.

ARTICLE

Cobalt/Polypyrrole Nanocomposites with Controllable Electromagnetic Properties

Haicheng Wang,^a Ning Ma^a, Zhiran Yan^a, Ling Deng^a, Jun He^{b*}, Yanglong Hou^c, Yong Jiang^a, and Guanghua Yu^{a*}

In this work, cobalt/polypyrrole (Co/PPy) nanocomposites were prepared via an in situ oxidation polymerization of pyrrole in an aqueous dispersion of Co nanoparticles (NPs). The Co/PPy nanocomposites showed good electromagnetic properties because of the coexistence of magnetic loss and dielectric loss to electromagnetic wave. The electromagnetic wave absorbing bandwidth (reflection loss < -10 dB) for Co/PPy (30 wt% in paraffin matrix) was located at 11.7~16.47 GHz at a thickness of 2 mm, and with a maximum reflection loss (around -33 dB) at 13.6 GHz. More interestingly, the electromagnetic wave absorbing property of the nanocomposites can be easily controlled by tuning the ratio of the two components in the composites. This better electromagnetic wave absorption may be attributed to the excellent electromagnetic match at corresponding resonance peaks for dielectric and magnetic loss. These magnetic nanoparticles/conducting polymer nanocomposites are great potential candidates for electromagnetic wave absorbent due to their excellent properties such as wide absorbing frequency, strong absorption, good compatibility, low density and controllable absorbing properties.

Introduction

Electromagnetic (EM) wave absorbing materials have been widely and continuously studied for their great potential for application in precise instrument, body-protecting and wave-absorbing coatings.¹⁻⁶ Generally, the EM radiation can be weakened by the absorbing materials with either magnetic loss⁷⁻¹⁰ or dielectric loss¹¹⁻¹² to EM waves. Conventional magnetic absorbers, including nano/sub micrometre iron particles,¹³ polycrystalline iron-fiber,¹⁴ Fe₃O₄,¹⁵ Fe/SiO₂ core-shell nanoflakes¹⁶ and Ni fibers,¹⁷ have been extensively studied due to their good performance and wide absorbing frequency. However, their applications are highly limited due to the disadvantages such as high specific gravity. For this purpose, electromagnetic wave absorbing materials with light-weight and high performance have drawn great attention to researchers recently¹⁸. Sun et al synthesized laminated magnetic graphene composite (Fe₃O₄/graphene) for EM wave absorbing, and found that the reflection loss (RL) of the as-prepared composite is below -10 dB (90% absorption) at 10.4–13.2 GHz with a coating layer thickness of 2.0 mm.¹⁹ Yang and coworkers prepared Fe@SiO₂ core-shell microcubes, and found that the reflection loss value of -54 dB could be obtained at 3.2 GHz with a thickness of 4.5 mm. The silica coated mesoporous iron microcubes significantly reduced the usage/thickness of silicon resin composite.²⁰ Another popular method to decrease the density of the materials and improve the absorbing performance is to composite the magnetic absorbers with polymeric matrixes to form composite materials. For example, Zheng et al prepared a new type of light-weight, high-performance polymeric composite foams by incorporating a hybrid structure of

graphene@Fe₃O₄ into the polyethyleneimine(PEI) matrix.²¹ The density of as-prepared foams was in the range of 0.28 to 0.40 g/cm³, and a high EMI SE (electromagnetic interference shielding effectiveness) of ~14.3-18.2 dB over a frequency range of 8-12 GHz can be obtained. Wang et al reported carbon nanocoils (CNC) coated with highly controlled magnetic materials, and found that the minimum RL of Fe₃O₄/Al₂O₃/CNCs with 6, 12, 24, and 36 nm Fe₃O₄ shells are -10.7, -18.4, -28.3, and -5.5 dB at 8.8, 10.9, 11.9, and 17.7 GHz, respectively.²² Ren et al summarized current progress on the modification of carbon nanotubes and their application in electromagnetic wave absorption but most of reported RL values were not better than -30 dB.²³

Furthermore, conductive polymers are being developed to prepare promising materials for wave absorbing due to their relatively high electrical conductivity and dielectric constant.²⁴ It is important that their association with magnetic nanoparticles may create nanocomposites with a higher shield efficiency because of the contribution of the magnetic loss, $\tan\delta_m (= \mu''/\mu')$ provided by the magnetic filler.²⁵ Moreover, conducting polymer-magnetic nanoparticle nanocomposites may be designed to work as signal-triggered materials with properties being modulated by the application of an external stimulus.²⁶ Shen et al fabricated double core-shell (Z-type barium ferrite/silica)@Polypyrrole composites, and a minimum reflection loss value of -19.65 dB is obtained for the composites with 66.67 wt% PPy with thickness of 2 mm.²⁷ Li et al reported polystyrene@polypyrrole@nickel (PS@PPy@Ni) composite microspheres, and found that the PS@P(Py-COOH)@Ni composite microspheres show the remarkable EM wave absorption property with the maximum reflection loss (around -20.06 dB) at 10.69 GHz.²⁸ Huang et al synthesized ternary composites of poly(3,4-ethylenedioxythiophene)-reduced graphene

oxide–Co₃O₄ (PEDOT–RGO–Co₃O₄), and found that the maximum reflection loss of PEDOT–RGO–Co₃O₄ could reach –51.1 dB at 10.7 GHz, and the bandwidth exceeding –10 dB was 3.1 GHz with absorber thickness of 2.0 mm.²⁹ Chen et al prepared ternary composites of expanded graphite/polyaniline microparticles/CoFe₂O₄(EG/PANI/CoFe₂O₄), and got the minimum reflection loss of -19.13 dB at 13.28 GHz and an available bandwidth of 5.94 GHz.³⁰ However, a ternary composite may be a little complicated for the control of the properties in real applications. To our best knowledge, there are still few reported literatures about the magnetite/conductive polymer composites.^{31–32} New types of nanocomposites with light-weight, strong absorption and wide absorbing frequency is still needed for further investigation of advanced absorbers.

In this paper, we prepared a relatively simple binary Co/PPy nanocomposite to develop a new EM absorbing composite material. Co nanoparticles were chosen as magnetic components, for their controllable crystal structure, particle size, shape, and tunable magnetic property.^{33–35} Meanwhile, polypyrrole(PPy) was chosen as electric component, for its well-controlled conductivity³⁶ and controllable dielectric loss³¹. Co/PPy nanocomposites are prepared via an insitu oxidation polymerization in an aqueous dispersion of Co nanoparticles, illustrated in Figure 1. As shown in Figure 1, Co nanoparticles are carried out with a chemical reduction procedure, in which the blue Co²⁺ complex was reduced to Co nanoparticles by lithium triethylborohydride. As-prepared Co NPs were dispersed steadily in nonpolar phase. However, it was hard to composite with PPy for Co NPs in this condition for their poor dispersity in aqueous phase. Therefore, the Co NPs should be hydrophilically modified. After the hydrophilic functionalization, the composition of Co NPs with polypyrrole was carried out by oxidative polymerization of pyrrole in aqueous media. It is shown by some measurements that this Co/PPy nanocomposite have a good electromagnetic wave absorbing performance with wide absorbing frequency, strong absorption, good compatibility and lower density.

Experimental

Materials.

Cobalt acetate (99%), oleic acid (97+%), benzyl ether (99%), triphenylphosphine (99%), lithium triethylborohydride (1M in THF), and pyrrole (99%) were purchased from Acros, mercaptoacetic acid (97+%) was obtained from Alfa Aesar. All chemicals were used without further purification unless stated. Other chemicals were obtained from Beijing Chemical Reagent Corporation and used without further purification unless stated.

Synthesis, surface modification of Co nanoparticles.

The synthesis procedure of Co nanoparticles followed the method reported by Sun et al.³⁷ In a typical experiment, cobalt acetate (1 mmol), oleic acid (1 mmol), and benzyl ether (20 mL) were mixed under argon and heated to 100 °C. Triphenylphosphine (3 mmol) was added and the mixture was then heated to 200°C. Benzyl ether superhydride solution (2 mL, 2 mmol superhydride) was injected during vigorously magnetic stirring. A color change from dark blue to black was then observed, indicating reduction of the blue Co²⁺ complex to form cobalt particles. The black solution was stirred at 200°C for 30 min and then cooled to room temperature. Particles were precipitated by adding ethanol to dispersion, followed by centrifuging. The precipitate was redispersed in 15 mL hexane with 200 µL of oleic acid to ensure stability.

Mercaptoacetic acid (0.5 mL) was used as polar ligand and added to the hexane dispersion of Co NPs to replace oleic acids on

the surface of Co NPs. After modification with mercaptoacetic acid, Co NPs can be transferred into stable dispersion in aqueous phase.

Preparation of Co/PPy nanocomposites.

Amount of sodium dodecyl benzene sulfonate (SDS, 0.2 g) and pyrrole monomer (Py, 2.0 mL) were mixed in deionized water. Co NPs in water solution was then added, and the mixture was ultrasonic stirred. Ammonium persulfate aqueous solution, which was cooled to 278K simultaneously, was added into the Co/Py solution. After keeping in situ polymerization for a few hours (6–8h), the Co/PPy nanocomposites were washed with deionized water, and then vacuum dried after suction filtration.

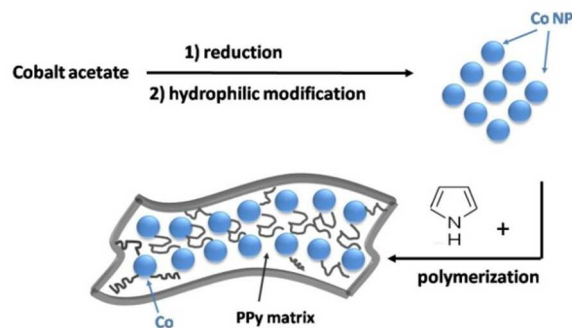


Figure 1. Schematic diagram of synthesis of Co/PPy composites.

Characterization of the nanoparticles and Co/PPy nanocomposites.

The morphology, crystal structure, and composition of the Co NPs were determined by High-resolution Transmission Electron Microscopy (HRTEM, FEI F30). STEM-EDS mapping was performed on a scanning transmission electron microscope (STEM, FEI TitanX) at 200 kV equipped with a SuperX windowless EDS detector. Temperature and field-dependent magnetization measurements were performed on a Physical Property Measurement System-Vibrating Sample Magnetometer (Quantum Design, PPMS).

Electromagnetic measurements.

The relative complex permittivity and permeability versus frequency were obtained by the coaxial reflection/transmission method using an Agilent 8722ES vector network analyzer in the frequency of 1–18 GHz. The cylindrical sample (with 3.00 mm inner diameter, 7.00 mm outer diameter and 2.00 mm thickness) was fabricated by uniformly mixing paraffin matrix with a certain amount of Co/PPy nanocomposite absorbers. Then the composite was pressed into cylindrical compacts. The transmission line theory was introduced to characterize the wave-absorbing properties, designated as reflection loss (*RL*).

Results and discussion

The as-synthesized Co nanoparticles were stabilized with oleic acid and form stable dispersion in organic media such as hexane, which allowed us to conduct the hysteresis loop measurements and TEM observation. As shown in Figure 2a), the obtained Co nanoparticles were monodispersed in the dispersion with the average diameter of about 10 nm. From the *M-H* curve measured at room temperature with a maximum magnetic field of 5 kOe, the Co NPs show some ferromagnetic property. The magnetic nanoparticles may contribute to magnetic loss for electromagnetic wave, which will result in an effect wave absorbing performance.¹⁸ The selected area electron diffraction (SAED), shown in Figure 2b), illustrated that the Co nanoparticles prepared was polycrystalline.

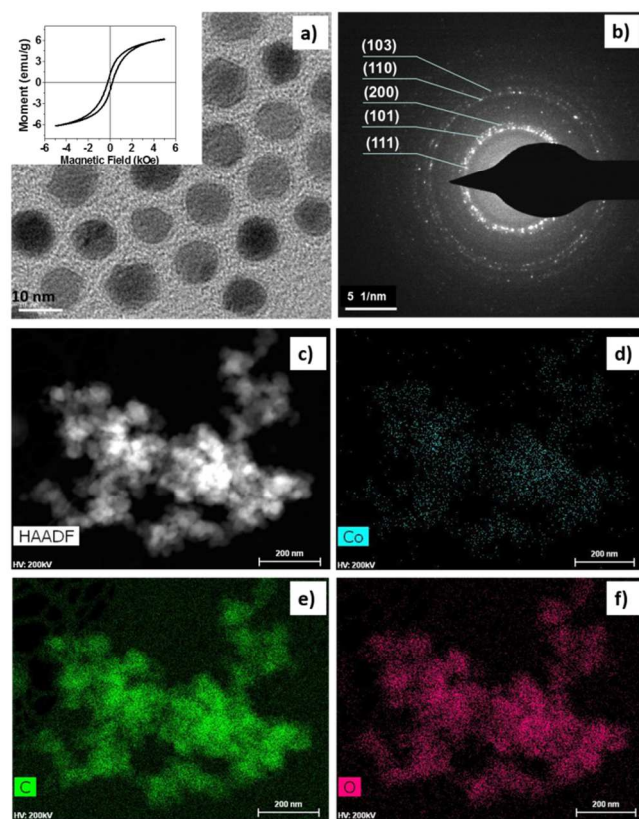


Figure 2. TEM photograph and M-H curve (a), SAED pattern (b) of prepared Co NPs ($T=300\text{K}$), and STEM-EDS element mapping of composites (c): cobalt (d), carbon (e), oxygen (f).

Up to now, Co nanoparticles with tunable properties and controllable shape or size were usually synthesized in organic solvents under a high temperature and stabilized with hydrophobic organic molecules.³⁸⁻⁴⁰ Therefore, the Co NPs need to be hydrophilically modified before composition with polypyrrole by oxidative polymerization, which is normally carried out in an aqueous media. In this purpose, mercaptoacetic acid was used as a capping agent to transfer Co NPs to aqueous solution. As-synthesized Co NPs were stabilized with oleic acids could be dispersed steadily in hexane, showing the Co NPs were hydrophobically functionalized. After adding mercaptoacetic acid, the Co nanoparticles precipitated from hexane, indicating the ligand replacement of Co NPs with mercaptoacetic acids instead of oleic acids. The hydrophilically modified Co NPs were purified by centrifugation. The obtained Co NPs could be well dispersed in deionized water and are suitable for further composition with PPy.

The Co/PPy nanocomposites were prepared by oxidative polymerization of pyrrole in presence of cobalt nanoparticles in aqueous media, and purified by filtration and washing with deionized water. The morphology of the Co/PPy nanocomposites and element mapping were observed by STEM. It can be seen from Figure 2(c) - 2(f) and Figure S1 that, Cobalt has a relatively even distribution in the Co/PPy nanocomposites. The good distribution of Co NPs will greatly contribute to the uniformity of the performance of the Co/PPy nanocomposites. From the FT-IR spectra (Figure S2), it can be seen that the absorption bands assigned to the stretching vibration of doped PPy, the deformation vibrations of C-H, and the stretching vibrations C-N, shifted to smaller wavenumbers after the

nanocomposition with Co nanoparticles. These shifts, especially the shift of C-N stretching vibrations (from 1319 to 1296 cm^{-1}) can prove the existence of the strong interaction between Co NPs and pyrrole moieties in PPy polymers.

What we are most interested in is the electromagnetic properties of the Co/PPy nanocomposites. For this reason, the electromagnetic parameters of the paraffin matrixes filled with Co/PPy were investigated by measuring relative complex permittivity, $\epsilon_r = \epsilon_r' + \epsilon_r''$, and permeability, $\mu_r = \mu_r' + \mu_r''$, in a frequency range of 1-18 GHz. Here, the real relative complex permittivity (ϵ_r') and the imaginary part (ϵ_r'') of relative complex permittivity represent the energy storage ability and loss ability, respectively. The tangent of dielectric loss can be expressed as $\tan\delta_\epsilon = \epsilon_r'' / \epsilon_r'$ and $\tan\delta_m = \mu_r'' / \mu_r'$, respectively. In fundamental theoretical research of absorbing materials, it is a common practice to measure the electromagnetic features (complex permittivity and permeability) by combining network analysis with transmission line theory.⁴¹⁻⁴²

The first tested sample was prepared by filling 20 wt% Co/PPy nanocomposites with paraffin matrixes and used for measurements of electromagnetic properties. Figure 3 (a)-d) illustrates $\epsilon(\epsilon', \epsilon'')$, $\tan\delta_\epsilon$, $\mu(\mu', \mu'')$, $\tan\delta_m$ at the frequency of 1-18 GHz, where ϵ' , ϵ'' mean the real and the imaginary part of the relative complex dielectric permittivity respectively, $\tan\delta_\epsilon$ means the dielectric dissipation factor, μ' and μ'' mean the real and the imaginary part of relative complex permeability respectively, and $\tan\delta_m$ means the magnetic dissipation factor. It can be seen that in the frequency range of 1-18 GHz, ϵ' located within the range of 8-18, ϵ'' located within the range of 4-8.6, and the dielectric dissipation factor, $\tan\delta_\epsilon$, was in the range of 0.42-0.58. The $\tan\delta_\epsilon$ decreases at first, getting a minimum value 0.426, and then increases to a maximum value 0.57 within 1-18 GHz. It may have an effective absorption to EM wave because of the ac and dc dielectric loss contribution of PPy.⁴³ The real relative complex permeability, μ' , is within the range of 0.89-1.02, and the imaginary part, μ'' , within -0.02~0.08. The magnetic dissipation factor, is within the range of -0.02~0.1, and shows a maximum value at 13.5 GHz. There are mainly four resonance peaks in Figure 3 d). The first resonance peak around 2GHz can be attributed to the Kittel natural resonance (the so-called uniform rotation) The others resonance peaks around 9GHz, 13GHz, 17 GHz, may be attributed to the exchange resonance.⁴⁴⁻⁴⁵ It indicates that Co nanoparticles had coexistence of natural resonance and exchange resonance, which may lead to an effective absorption to EM wave at lower and higher frequencies.

On the basis of the model of metal backplane, the RL of the sample is determined from the measured relative complex permeability and permittivity according to the following equations:

$$RL/\text{dB} = 20 \log |(Z_{in} - 1)/(Z_{in} + 1)| \quad (1)$$

$$Z_{in} = \sqrt{\frac{\mu}{\epsilon}} \tanh(j2\pi\sqrt{\mu\epsilon}fd/c) \quad (2)$$

where Z_{in} , d , and μ are the normalized input impedance, thickness, and permeability of the material, respectively; c is the light velocity in vacuum; and f is the microwave frequency.⁴⁶⁻⁴⁷ When the RL is smaller than -10 dB, only 10% of the microwave energy is reflected while 90% of that is absorbed. The corresponding frequency range over which the RL is smaller than -10 dB is defined as the effective absorption bandwidth. The RL value of -20 dB is comparable to 99%

of incident electromagnetic wave absorption, and thus $RL < -20$ dB is considered as a threshold value for the electromagnetic wave absorption application.

It is well known that the relative permeability and permittivity of absorbing materials determine the electromagnetic wave-absorbing characteristics, such as the maximal RL value and corresponding frequencies, as well as the absorbing bandwidth. It has been proven that directly-measured reflection loss is nearly identical to the calculated one, due to the same underlying physical origin.⁴⁸⁻⁵⁰ Thus, the RL of an absorbing material backed on a conductor can be calculated using the relative complex permeability and permittivity at a given frequency (f) and thickness (d) according to the transmit-line theory.⁴¹

Figure 3 e) shows the calculated RL of paraffin composites with 20 wt% Co/PPy at different thickness (1~10 mm). The reflection loss values less than -10 dB are obtained in all the samples when the composites thickness is 2-10 mm. The nanocomposite shows a maximum RL value -17 dB at 12.9 GHz with a thickness of 2 mm, and the electromagnetic absorbing bandwidth ($RL < -10$ dB) is 4.8 GHz. At a thickness of 3 mm, the composite shows a maximum RL value -17.5 dB, and the absorbing bandwidth is 2.72 GHz. The better absorption to EM wave at wider frequency range could be resulted from a better match of dielectric and magnetic loss at S-band (2–4GHz), C-band (4–8 GHz) and X-band (8–12GHz). The maximum RL peaks move to lower frequency with increasing the thickness of the composites. This can be explained by the equation $f = c/2\pi\mu_r d$, in which μ_r is imaginary part of relative permeability (μ_r), d is the thickness and f is the frequency. The corresponding frequency can be considered as an inverse function of thickness.^{27,51} Therefore, it can be easily understood that the corresponding frequency decreases with the increasing of sample thickness. It can be indicated that the absorbing performance is controllable, and the absorbing frequency width can be broadened by using multilayer wave absorbing nanocomposites.

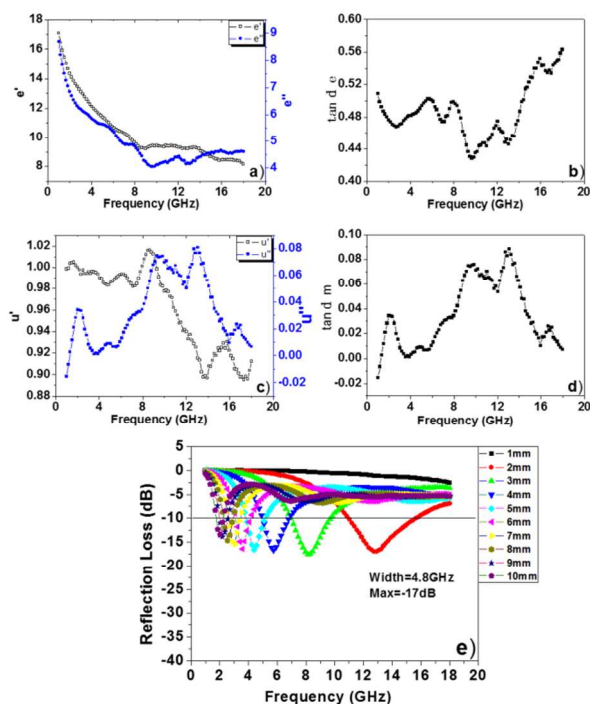


Figure 3. $\epsilon(\epsilon', \epsilon'')$ (a), $\tan\delta_e$ (b), $\mu(\mu', \mu'')$ (c), $\tan\delta_m$ (d) of paraffin composites filled with 20wt%Co/PPy, and calculated reflection loss of paraffin composites with different thickness(e).

We are curious if the content of Co/PPy nanocomposites can result in different electromagnetic properties of the sample. Therefore, another sample with content of 30 wt% Co/PPy was prepared and investigated. Figure 4 shows $\epsilon(\epsilon', \epsilon'')$, $\tan\delta_e$, $\mu(\mu', \mu'')$, $\tan\delta_m$, and the calculated RL of paraffin composites filled with 30wt% Co/PPy. We can see that, in the frequency range of 1-18 GHz, ϵ' is within the range of 7.83-14.58, ϵ'' is within the range of 3.25-9.06, and the dielectric dissipation factor, $\tan\delta_e$, is within the range of 0.4-0.623. The real relative complex permeability, μ' , is within the range of 0.915-1.0, and the imaginary part, μ'' , is within -0.026-0.053. The magnetic dissipation factor, is within the range of -0.03-0.06. Figure 4 e) shows that the calculated RL values less than -10 dB are obtained in all the samples when the composites thickness is 2-10 mm. The composite shows a maximum RL value -33 dB at 13.6 GHz with a thickness of 2 mm, and the electromagnetic absorbing bandwidth ($RL < -10$ dB) is 4.8 GHz. The improvement of absorption to EMW may due to the increase of ratio of Co/PPy in the paraffin, since there are both dielectric and magnetic loss to EM wave. The maximum RL peaks move to low frequency with increasing the thickness of the samples. The Co/PPy nanocomposites can have an effective absorbing ability to EM wave, and the absorbing performance is controllable.

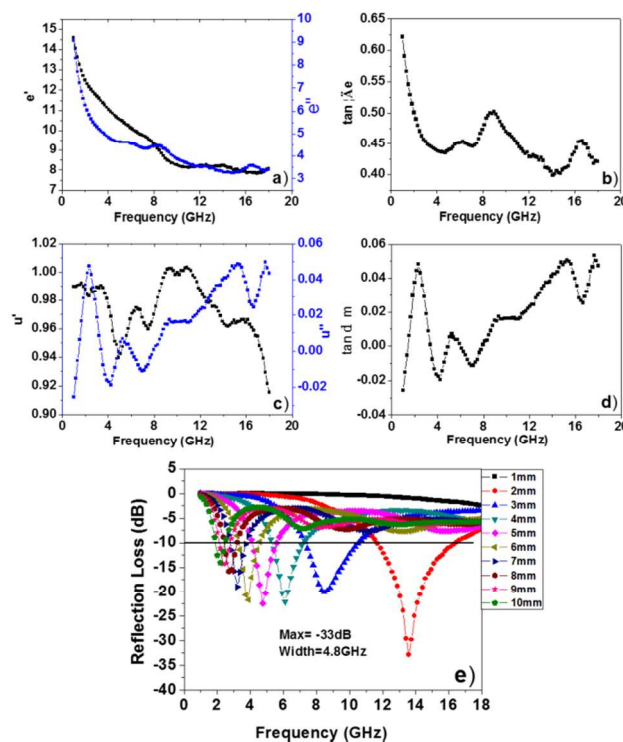


Figure 4. $\epsilon(\epsilon', \epsilon'')$ (a), $\tan\delta_e$ (b), $\mu(\mu', \mu'')$ (c), and $\tan\delta_m$ (d) of paraffin composites filled with 30wt% Co/PPy, and calculated reflection loss of paraffin composites with different thickness(e).

More interestingly, it is found that the electromagnetic properties and reflection loss of composite samples can also be influenced by the content of Co NPs in the Co/PPy nanocomposites. To realize this, Co/PPy nanocomposites with different Co contents were prepared by adjusting the ratio between Co NPs and pyrrole monomer in the polymerization. As indicated in Figure 5 a)-b), most of the composites with different thickness showed the reflection loss beyond -10 dB. Comparing with the sample shown in Figure 3 to 4 (Co=0.11g), it can be found from Figure 6 that, reducing Co content

can make the wave absorption performance of composite sample moving to lower wave absorbing frequency range, while enlarging Co content could result in higher frequency of wave absorption performance of the tested sample. As enlarging Co content from 0.05g to 0.155g, the frequency corresponding to the maximum reflection loss can increase from 8.5 GHz to 16.5 GHz. It can be understood that, when increasing the content of Co, the density of Co nanoparticles will be increased, and then there will be more magnetic moments in the Co particles which was responsible for the exchange resonance in higher frequency range, so the composite will have a better absorption to EM wave at higher frequency range. Besides, it is also shown in Figure 5 and Figure 6 that, the RL value of composites with more cobalt content had been lowered. This case might be due to the increase of conductivity of the composites as increasing the cobalt content. This could decrease the dielectric properties of the composites, which would lower the reflection loss.

Different ratio of cobalt to PPy, means different dielectric loss and magnetic loss of electromagnetic wave. Therefore, composite materials with different wave absorption performance can be obtained by adjusting the proportion of cobalt nanoparticles and PPy. Therefore, it can be concluded that this is an effective way to control and regulate electromagnetic wave absorbing performance of the nanocomposites by optimizing the content of Co nanoparticles and the thickness of the Co/PPy nanocomposites, which may develop a new broadband EM absorbing material.

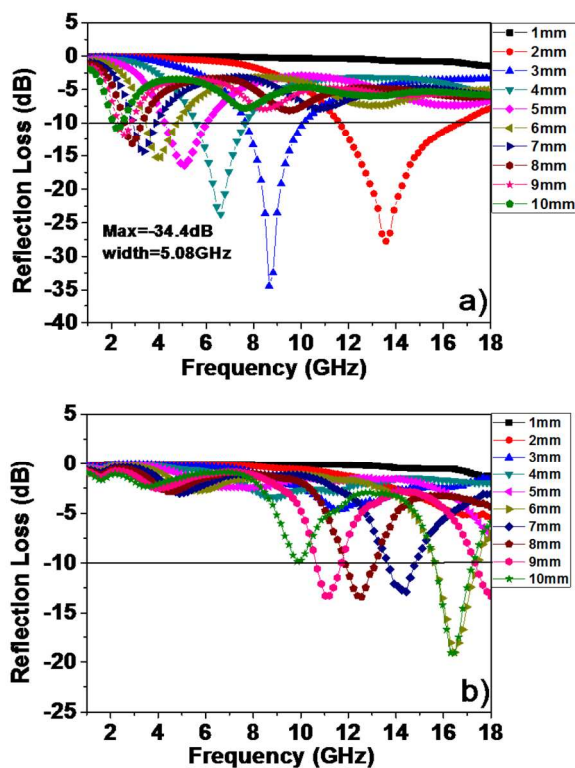


Figure 5. Calculated reflection loss of paraffin composites (Co/PPy= 30 wt%) with different Co content. a) Co=0.05g, b) Co=0.155g.

The composition of Co NPs and PPy polymers could bring effective improvement and controlling on the electromagnetic properties of the nanocomposites. By this nanocomposition method, it is convenient to solve the dispersion problem of

magnetic nanoparticles in the polymer matrixes by ligand exchange. The in-situ polymerization procedure is more beneficial to the interfacial combination of magnetic Co nanoparticles and conductive PPy polymers, which may induce more interfacial polarization, thus resulting in the great magnetic loss and dielectric loss to electromagnetic waves. Therefore, an effective controllable electromagnetic wave absorbing performance could be realized by optimising the proportion of magnetic Co nanoparticles and PPy polymer in the nanocomposites.

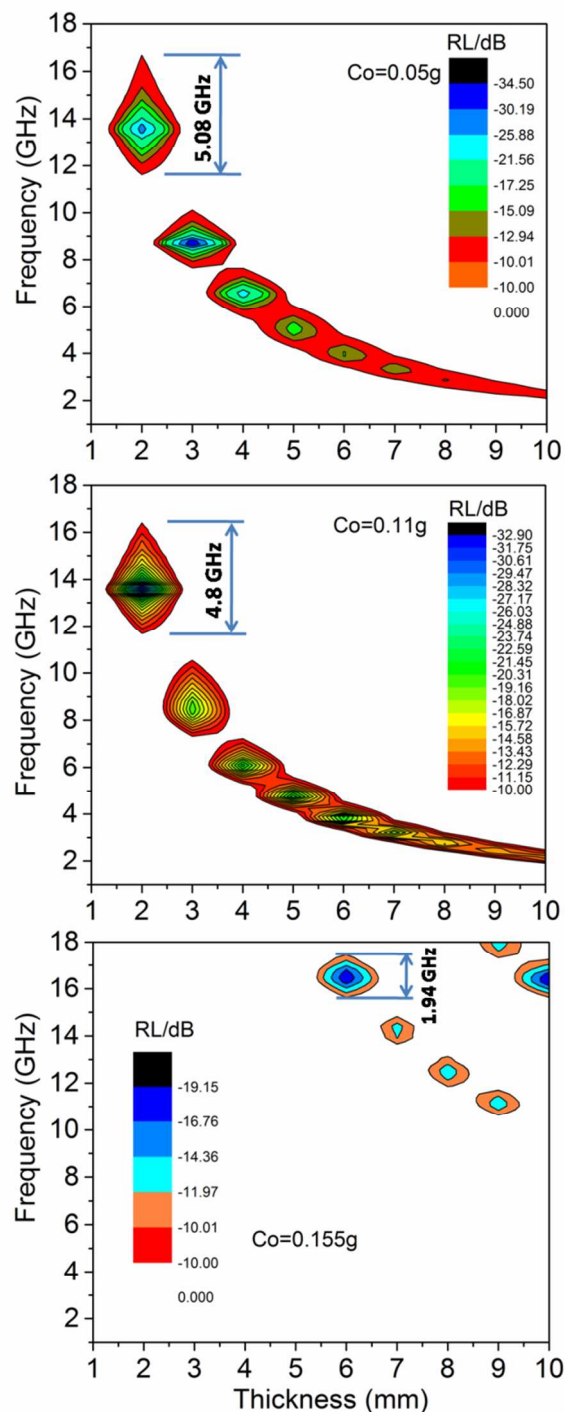


Figure 6. Contour map of the bandwidth with RL < -10 dB (90%)

absorption) as a function of the absorbent thickness with different Co NPs content. a) Co=0.05g, b) Co=0.11g, c) Co=0.155g.

Conclusions

In summary, Co/PPy nanocomposites were prepared by in situ polymerization of pyrrole in an aqueous dispersion of Co NPs. The electromagnetic properties testing indicated that these Co/PPy nanocomposites had both magnetic loss and dielectric loss to electromagnetic wave, which would contribute to controllable EM wave absorbing performance. The EM wave absorbing bandwidth ($RL < -10$ dB) for Co/PPy (30 wt%) was located at 11.7–16.47 GHz at a thickness of 2 mm, and with a maximum reflection loss (around -33 dB) at 13.6 GHz. Besides, the content of Co NPs will also have a great effect on the wave absorbing performance. Less cobalt content can make the wave absorption performance of composite sample moving to lower absorbing frequency range, while enlarging Co content could result in higher frequency of wave absorption performance. These Co/PPy nanocomposites have good properties like wide absorbing frequency, strong absorption, good compatibility, low density, small thickness. The present research is believed, hopefully, to be a competitive way to manufacture novel controllable and effective broadband electromagnetic wave absorbing materials.

Acknowledgements

The authors are grateful for the financial support from the National Natural Science Foundation of China (51101013, 21104004, 51371055), Beijing Municipal Natural Science Foundation (2132049), and the Fundamental Research Funds for the Central Universities (FRF-TP-14-012A2).

Notes and references

^aSchool of Materials Science and Engineering, University of Science and Technology Beijing, Beijing, 100083, P.R.China. E-mail: hcwang@mater.ustb.edu.cn, ghyu@mater.ustb.edu.cn

^bInstitute of Functional Materials, Central Iron & Steel Research Institute, Beijing, 100081, P.R.China. E-mail: hejun@cisri.com.cn

^cDepartment of Advanced Materials and Nanotechnology, College of Engineering, Peking University, Beijing, 100871, P.R.China.

- Z. J. Wang, L. N. Wu, J. G. Zhou, W. Cai, B. Z. Shen and Z. H. Jiang, *J. Phys. Chem. C*, 2013, **117**, 5446–5452.
- S. I. Ohkoshi, S. Kuroki, S. Sakurai, K. Matsumoto, K. Sato and S. Sasaki, *Angew. Chem., Int. Ed.*, 2007, **46**, 8392–8395.
- G. X. Tong, F. F. Du, L. J. Xiang, F. T. Liu, L. L. Mao and J. G. Guan, *Nanoscale*, 2014, **6**, 778–787.
- Y. P. Duan, Z. Liu, Y. H. Zhang and M. Wen, *J. Mater. Chem. C*, 2013, **1**, 1990–1994.
- C. Wang, X. J. Han, P. Xu, X. L. Zhang, Y. C. Du, S. R. Hu, J. Y. Wang and X. H. Wang, *Appl. Phys. Lett.*, 2011, **98**, 072906.
- J. H. Shen, K. Y. Chen, L. C. Li, Y. Ding, J. B. Li and W. Q. Kong, *Sci China Tech. Sci.*, 2014, **57**, 1858–1864.
- G. B. Sun, B. X. Dong, M. H. Cao, B. Q. Wei and C. W. Hu, *Chem. Mater.*, 2011, **23**, 1587–1593.
- C. Yan, X. Q. Cheng, Y. Zhang, D. Z. Yin, C. H. Gong, L. G. Yu, J. W. Zhang and Z. J. Zhang, *J. Phys. Chem. C*, 2012, **116**, 26006–26012.
- S. T. Kim and S. S. Kim, *IEEE Trans. Magn.*, 2012, **48**, 3494–3497.
- Y. P. Duan, Z. Liu, H. Jing, Y. H. Zhang and S. Q. Li, *J. Mater. Chem.*, 2012, **22**, 18291–18299.
- Y. C. Qing, W. C. Zhou, F. Luo and D. M. Zhu, *Carbon*, 2010, **48**, 4074–4080.
- Y. J. Chen, G. Xiao, T. S. Wang, Q. Y. Ouyang, L. H. Qi, Y. Ma, P. Gao, C. L. Zhu, M. S. Cao and H. B. Jin, *J. Phys. Chem. C*, 2011, **115**, 13603–13608.
- X. A. Fan, J. G. Guan, W. Wang and G. X. Tong, *J. Phys. D: Appl. Phys.*, 2009, **42**, 075006.
- X. L. Yu, X. C. Zhang, H. H. Li and H. H. He, *Mater. Des.*, 2002, **23**, 51–57.
- S. B. Ni, S. M. Lin, Q. T. Pan, F. Yang, K. Huang and D. Y. He, *J. Phys. D: Appl. Phys.*, 2009, **42**, 055004.
- L. G. Yan, J. B. Wang, X. H. Han, Y. Ren, Q. F. Liu and F. S. Li, *Nanotechnology*, 2010, **21**, 095708.
- C. H. Gong, J. W. Zhang, X. F. Zhang, L. G. Yu, P. Y. Zhang, Z. S. Wu and Z. J. Zhang, *J. Phys. Chem. C*, 2010, **114**, 10101–10107.
- D. P. Sun, Q. Zou, Y. P. Wang, Y. J. Wang, W. Jiang and F. S. Li, *Nanoscale*, 2014, **6**, 6557–6562.
- X. Sun, J. P. He, G. X. Li, J. Tang, T. Wang, Y. X. Guo and H. R. Xue, *J. Mater. Chem. C*, 2013, **1**, 765–777.
- Z. H. Yang, Z. W. Li, L. H. Yu, Y. H. Yang and Z. C. Xu, *J. Mater. Chem. C*, 2014, **2**, 7583–7588.
- B. Shen, W. T. Zhai, M. M. Tao, J. Q. Ling and W. G. Zheng, *ACS Appl. Mater. Interfaces*, 2013, **5**, 11383–11391.
- G. Z. Wang, Z. Gao, S. W. Tang, C. Q. Chen, F. F. Duan, S. C. Zhao, S. W. Lin, Y. H. Feng, L. Zhou, and Y. Qin, *ACS Nano*, 2012, **6**, 11009–11017.
- F. J. Ren, H. J. Yu, L. Wang, M. Saleem, Z. F. Tian and P. Fren, *RSC Adv.*, 2014, **4**, 14419–14431.
- L. G. Paterno, M. A. G. Soler, F. J. Fonseca, J. P. Sinnecker, E. H. C. P. Sinnecker, E. C. D. Lima, M. A. Novak and P. C. Morais, *J. Phys. Chem. C*, 2009, **113**, 5087–5095.
- Z. Z. Wang, B. Hong, J. Liu, T. Sun and X. L. Wu, *J. Magn. Magn. Mater.*, 2008, **320**, 2132–2139.
- W. C. Zhou, X. J. Hu, X. X. Bai, S. Y. Zhou, C. H. Sun, J. Yan and P. Chen, *ACS Appl. Mater. Interfaces*, 2011, **3**, 3839–3845.
- J. H. Shen, K. Y. Chen, L. C. Li, W. X. Wang and Y. Jin, *J. Alloys Comp.*, 2014, **615**, 488–495.
- W. Z. Li, T. Qiu, L. L. Wang, S. S. Ren, J. R. Zhang, L. F. He and X. Y. Li, *ACS Appl. Mater. Interfaces*, 2013, **5**, 883–891.
- P. B. Liu, Y. Huang and X. Sun, *ACS Appl. Mater. Interfaces*, 2013, **5**, 12355–12360.
- K. Y. Chen, C. Xiang, L. C. Li, H. S. Qian, Q. S. Xiao and F. Xu, *J. Mater. Chem.*, 2012, **22**, 6449–6455.
- P. Xu, X. J. Han, C. Wang, D. H. Zhou, Z. S. Lv and A. H. Wen, *J. Phys. Chem. B*, 2008, **112**, 10443–10448.
- P. Montoya, F. Jaramillo, J. Calderon, S. Torresi and R. M. Torresi, *Electrochim. Acta*, 2010, **55**, 6116–6122.
- A. Z. Michael, L. V. Michael, S. R. Judy, S. Martin and G. S. P. Timothy, *Chem. Mater.*, 2007, **19**, 6597–6604.
- V. F. Puentes, K. M. Krishnan and A. P. Alivisatos, *Science*, 2001, **291**, 2115–2117.
- V. F. Puentes, P. Gorostiza, D. M. Aruguete, N. G. Bastus and A. P. Alivisatos, *Nat. Mater.*, 2004, **3**, 263–268.

- 36 M. Wysocka-Żołopa, E. Grądzka, K. Szymański and K. Winkler, *Thin Solid Films*, 2013, **548**, 44–51.
- 37 S. H. Sun and C. B. Murray, *J. Appl. Phys.*, 1999, **85**, 4325–4330.
- 38 G. S. Chaubey, C. Barcena, N. Poudyal, C. B. Rong, J. M. Gao, S. H. Sun and J. P. Liu, *J. Am. Chem. Soc.*, 2007, **129**, 7214–7215.
- 39 B. Y. Kim, I. B. Shim, Z. O. Araci, S. S. Saavedra, O. L. A. Monti, N. R. Armstrong, R. Sahoo, D. N. Srivastava and J. Pyun, *J. Am. Chem. Soc.*, 2010, **132**, 3234–3235.
- 40 P. Y. Keng, B. Y. Kim,; I. B. Shim,; R. Sahoo, P. E. Veneman, N. R. Armstrong, H. Yoo, J. E. Pemberton, M. M. Bull, J. J. Griebel, E. L. Ratliff, K. G. Nebesny and J. Pyun, *ACS Nano*, 2009, **3**, 3143–3157.
- 41 C. H. Gong, J. W. Zhang, C. Yan, X. Q. Cheng, J. W. Zhang, L. G. Yu, Z. H. Jin and Z. J. Zhang, *J. Mater. Chem.*, 2012, **22**, 3370–3376.
- 42 W. B. Weir, *Proc. IEEE*, 1974, **62**, 33–36.
- 43 V. T. Truong, S. Z. Riddell and R. F. Muscat, *J. Mater. Sci.*, 1998, **33**, 4971–4976.
- 44 H. Wang, Y. Y. Dai, W. J. Gong, D. Y. Geng, S. Ma, D. Li, W. Liu and Z. D. Zhang, *Appl. Phys. Lett.*, 2013, **102**, 223113.
- 45 H. Wang, H. H. Guo, Y. Y. Dai, D. Y. Geng, Z. Han, D. Li, T. Yang, S. Ma, W. Liu and Z. D. Zhang, *Appl. Phys. Lett.*, 2012, **101**, 083116.
- 46 L. Kong, X. W. Yin, Y. J. Zhang, X. Y. Yuan, Q. Li, F. Ye, L. F. Cheng and L. T. Zhang, *J. Phys. Chem. C*, 2013, **117**, 19701–19711.
- 47 P. A. Miles, W. B. Westphal and A. Von Hippel, *Rev. Mod. Phys.*, 1957, **29**, 279–307.
- 48 J. Guan, Z. Li, F. Mou, G. Tong and W. Wang, *J. Mater. Chem.*, 2010, **20**, 1676–1682.
- 49 Y. Naito and K. Suetake, *IEEE Trans. Microwave Theory Tech.*, 1971, **19**, 65–72.
- 50 C. K. Cui, Y. C. Du, T. H. Li, X. Y. Zheng, X. H. Wang, X. J. Han and P. Xu, *J. Phys. Chem. B*, 2012, **116**, 9523–9531.
- 51 P. Xu, X. J. Han, J. J. Jiang, X. H. Wang, X. D. Li and A. H. Wen, *J. Phys. Chem. C*, 2007, **111**, 12603–12608.